Assessment and validation of prestress loss prediction models using real-time prestress loss measurements

Alla Eddine Acheli, Hema Jayaseelan, Bruce W. Russell, Walter Peters, and Chris Filip

- This study investigates prestress loss measured on precast, prestressed concrete bridge beams for a bridge in Oklahoma. The research examines the effects of mild reinforcing steel in the bottom flange of precast concrete girders and the alternative prestressing pattern on the prestressing losses of pretensioned bridge girders.
- Using solar powered batteries, a structural monitoring system has been providing an ongoing stream of data since beam fabrication and will continue through the service life of the bridge.
- In addition to the measured data, the prestress losses were predicted at the girder midspan using five different methods for computing prestress loss.
- Data show that current equations overestimate the concrete elastic modulus at early ages, leading to an underprediction of elastic shortening losses.
- Results show that prestress losses are reduced by incorporating a combination of fully tensioned top strand plus mild steel in the bottom flanges of the bridge girder.

This paper investigates prestress losses measured on precast, prestressed concrete bridge beams fabricated and built for the State Highway 4 (SH 4) bridge over the North Canadian River in Canadian County, Okla. The SH 4 bridge consists of 15 spans; each span is nominally 100 ft (30 m) in length and supported by four Type IV girders made composite with the deck slab. Each of the 15 spans featured different reinforcement details at end regions and at midspan. Altogether, 60 pretensioned concrete bridge beams were fabricated and erected as part of the SH 4 bridge.

This paper's principal purpose is to experimentally examine the impacts of the inclusion of mild-steel reinforcement as primary reinforcement and alternative prestressing strand patterns to assess the effects on prestress losses and beam camber. The research experimentally examines the effects of including mild reinforcing steel in the bottom flange of precast concrete girder and the alternative prestressing pattern on the prestressing losses of pretensioned bridge girders. This paper also examines different methods for computing prestress losses on five different cross-section designs. Methods for computing losses included the *PCI Design Handbook: Precast and Prestressed Concrete* method, both the refined and approximate methods from the American Association of State Highway and Transportation Officials' *AASHTO LRFD Bridge Design Specifications*,[1] and the Jayaseelan time-step method.[2]

Two of the 60 prestressed girders were instrumented in end regions and midspans with vibrating wire gauges, bonded foil strain gauges, and thermocouples with continuous monitoring from the time they were fabricated to the current date.

Background

In recent years, self-consolidating concrete (SCC) use has increased significantly over conventional concrete mixtures. SCC (or concrete variations based on SCC principles) is widely used in the present-day fabrication of prestressed concrete bridge beams. SCC can be used to produce durable concrete with hardened concrete properties sufficient for use in bridges and other heavy construction projects. Okamura first proposed this type of concrete in 1986.[3] Since then, the use of SCC has increased rapidly in North America, particularly in the precast concrete industry, where it has been employed extensively in the United States since the mid-2000s. SCC is widely used to manufacture precast concrete elements for bridges.[4] There are several advantages to using SCC. Because SCC does not require consolidation and is generally self-leveling, it significantly minimizes labor and equipment costs.[5] SCC improves workability because it is fluid enough to flow into forms and around reinforcement without vibration. SCC has low segregation and high flowability, making its placement uniform and consistent. SCC also exhibits compressive strengths comparable to that of conventional concrete.[6] The essential components of SCC are the same as those of traditional concrete. However, SCC usually consists of smaller coarse-aggregate particles and smaller quantities of coarse aggregate (for a given concrete mixture proportions).[7] Also, SCC often requires special gradations of aggregates. Because of these changes, SCC has a greater paste volume than that of conventional concrete.

Research has shown that the elastic modulus for SCC is generally lower than that of conventional concrete with similar compressive strength. This is largely attributed to the larger paste volume in SCC.[8] Literature indicates that SCC's modulus of elasticity is about 10% to 15% lower than that of conventional concrete with a similar compressive strength.[5,9] Because SCC has a smaller modulus of elasticity, many researchers have reported that the prestress losses are higher than those predicted by the current models.[10] Underpredicting the elastic modulus of concrete for SCC leads to elastic shortening losses larger than those predicted by current models. Creep and shrinkage losses may also be underpredicted, and these time-dependent losses also depend on the concrete's paste content.

In addition to SCC's lower elastic modulus, Bonen and Shah note that the shrinkage of SCC is greater than that of conventional concrete.[11] Similar conclusions can be drawn regarding creep because SCC incorporates less coarse aggregate volume and smaller coarse aggregate sizes than non-self-consolidating concrete mixtures. However, research on the effects of creep in SCC is limited. None of the creep and shrinkage models can include a broad range of SCCs that are applied in the market today.[12]

The most common method to measure prestress losses is to compute them from direct strain measurement of concrete.[13] Other researchers have attempted to infer prestress losses from other measurements. These include the natural frequencies of the structure,[14] the magnetic permeability of the prestressing strands,[15] and the stress wave velocity in acoustoelastic methods.[16] Baran et al.[17] experimentally compared different methods for determining losses in pretensioned concrete girders. Baran et al. concluded that the most effective method was the use of vibrating wire gauges embedded in the concrete or attached to an exposed strand. Furthermore, as detailed in a report on estimating prestress losses by joint American Concrete Institute (ACI)-American Society of Civil Engineers (ASCE) Committee 423,[18] most successful field applications and large-scale laboratory experiments for monitoring prestress losses are based on strain measurements using strain sensors installed on the prestressing strands or other nonprestressed reinforcement embedded in the concrete. The strain measurements accurately represent the stress applied to the concrete.[18]

Jayaseelan and Russell[2] investigated the inclusion of fully tensioned top strands and the effects on prestress losses and cambers. The authors analyzed five different pretensioned, prestressed beam designs, including a base case with no top strand and no mild steel, two cases with varying amounts of mild steel, and two cases that included both mild steel and varying amounts of fully tensioned top strands. The authors developed a prestress loss prediction model known as the Jayaseelan time-step method, which breaks down time-dependent changes in both concrete strength and elastic modulus using the ACI 209R Eq. (2-1) framework.[19] The research compared the prestress losses using the *PCI Design Handbook* methods, the 2014 AASHTO LRFD specifications' approximate and refined methods, and the Jayaseelan time-step method. The Jayaseelan time-step method also computed the camber using beam mechanics. Jayaseelan and Russell[2] reported, based on analysis alone, that the inclusion of mild steel and fully tensioned top prestressing strands acts to reduce prestress losses and cambers compared with the base case, which contained neither mild steel nor fully tensioned top strands.

Methodology

Two of the 60 prestressed concrete girders for the SH 4 bridge were instrumented with vibrating wire strain gauges (VWSGs) and thermocouples at midspans and end regions. For the purposes of this paper, only the instruments at midspan are considered as they pertain to prestress losses at midspan. The instrumentation was attached to data acquisition systems that were made part of a solar-powered structural monitoring system that allowed continuous measurements around the clock. The data presented in this paper come from those systems.

Figure 1 shows the SH 4 bridge over the North Canadian River. The typical cross section of the bridge is shown in **Fig. 2**.

Figure 1. State Highway 4 bridge over the North Canadian River, Canadian County, Okla. (view looking north-northwest).

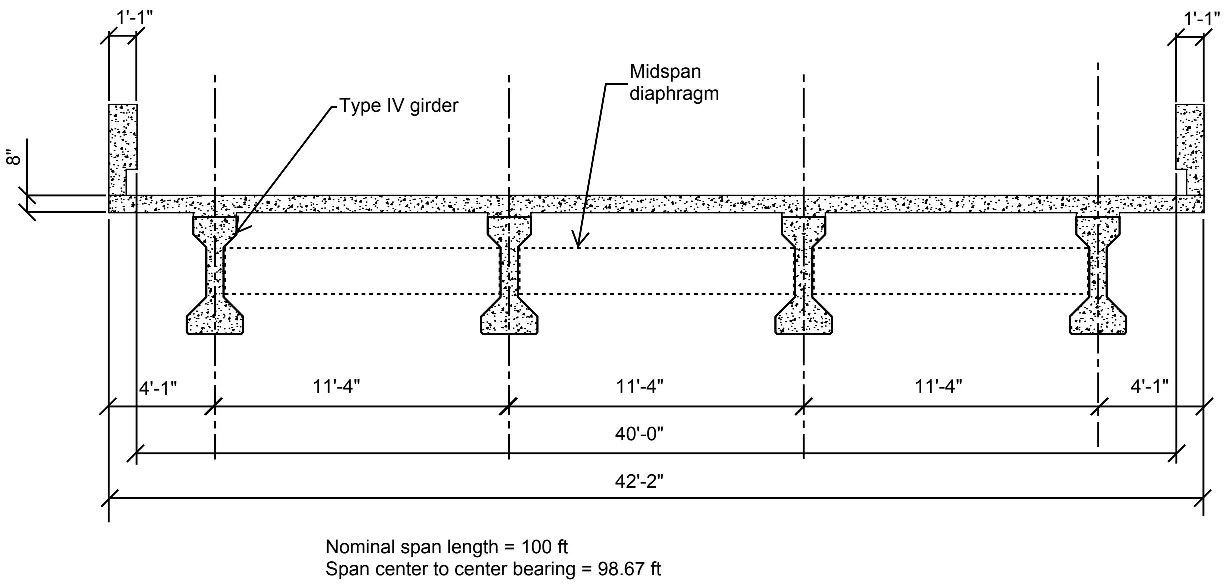

Figure 2. Cross section of State Highway 4 bridge. Note: 1" = 1 in. = 25.4 mm; 1' = 1 ft = 0.305 m.

Each of the 15 nominal 100 ft (30 m) spans contained different reinforcement patterns at midspan. The construction of the SH 4 bridge employed four different primary reinforcement details and included differences in both prestressing strand patterns and mild reinforcement. Primary reinforcement details are shown in **Fig. 3** and the variations are summarized in **Table 1**. All strands are 0.6 in. diameter.

This paper examines the effects of these variations in reinforcement at midspan, principally by physical measurement of concrete strains. The differences in prestressing strand pattern, plus the introduction of mild steel in the bottom flange, were expected to affect both prestress losses and measured beam cambers. The designs for SH 4 included four different primary reinforcement details. These include details A through D

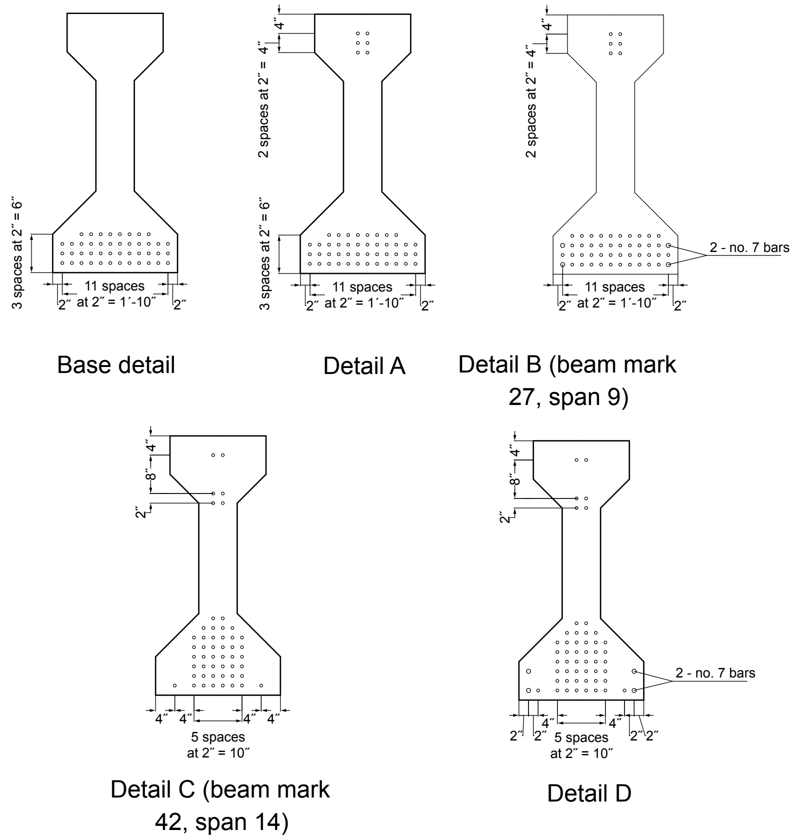

Figure 3. Primary reinforcement details for Type IV girders on the State Highway 4 bridge. Note: No. 7 = 22M; 1” = 1 in. = 25.4 mm.

Table 1. Prestressing strand patterns and longitudinal mild steel reinforcement

Type	Total number of strands	Number of top strands	Prestressed eccentricity e,* in.	Prestressed moment F_{pj}† × e, kip-in.	Area of mild steel, in.^{2}
Base detail	44	0	19.0	38,736	0.00
Detail A	50	6	14.0	30,760	0.00
Detail B	48	6	13.4	28,264	2.40
Detail C	50	6	11.9	26,146	0.00
Detail D	50	6	11.6	25,487	2.40

Note: e = eccentricity of the prestressing strand; F_{pj} = prestress jacking force. 1 in. = 25.4 mm; 1 in.^{2} = 645.2 mm^2; 1 kip-in. = 0.11298 kN-m; 1 ksi = 6.895 MPa.

*Based on gross cross-section properties.

†Jacking stress of 202.5 ksi is used for computations for prestressed moment.

(Table 1). The base detail included neither fully tensioned top strands nor mild reinforcement as longitudinal reinforcement at midspan. All the details were modeled for stresses, strains, and prestress losses, but physical measurements were made only on span 9 (detail B) and span 14 (detail C).

Figure 3 displays the strand patterns and mild-steel reinforcement layout for each cross section. Of these cross sections, only detail B (beam mark 27) and detail C (beam mark 42) were instrumented and prestress losses were measured from strain gauges. The following descriptions summarize the cross sections:

- Base detail: This detail was modeled for comparison purposes only. The strand pattern is typical for many states that do not use fully tensioned top strands.
- Detail A includes fully tensioned top strands to help control concrete stresses in end regions. Detail A is a representative strand pattern for pretensioned girder bridges in Oklahoma.
- Detail B matches detail A but includes four no. 7 (22M) reinforcing bars located in the bottom flange that help reduce creep strains. The reinforcement and strand pattern in detail B were used in fabrication of beam mark 27.
- Detail C is an alternative prestressing pattern that distributes prestressing forces through the depth of the cross section. Detail C effectively raises the center of gravity of the prestressing strands and reduces the prestress eccentricity more than detail A or B. The reinforcing pattern in detail C was used in fabrication of beam mark 42.
- Detail D matches the prestressing pattern from detail C but includes four no. 7 (22M) bars as primary reinforcement.

All 60 of the prestressed concrete Type IV girders fabricated for the SH 4 bridge incorporate the use of fully tensioned top strands. Fully tensioned top-strand patterns have been used in Oklahoma since 1997 for the express purposes of controlling stresses in end regions and deploying straight strand patterns instead of draping or harping.[20] Since that time, more than 800 precast, prestressed concrete bridges have been built with bridge girders that include fully tensioned top strands. It is safe to say that the State of Oklahoma, including both the Oklahoma Department of Transportation (ODOT) and Oklahoma Turnpike Authority, possesses three full decades of experience using fully tensioned top strands with good outcomes and few problems encountered. The use of fully tensioned top strands reduces both the number of debonded strands and the length required for debonding. All of the fully tensioned top strands are straight and are not draped.

Concrete mixture proportions conformed to Class P specification of the ODOT Standard Specifications for Highway Construction.[21] The four girders for span 9 were cast in the same prestressing bed on April 23, 2020. The four prestressed girders in span 14 were cast in the same prestressing bed on April 27, 2020. The design release strength was 7500 psi (51,700 kPa) and the design 28-day strength was 10,000 psi (68,950 kPa). The cast-in-place concrete deck on SH 4 conformed to ODOT Class AA with a specified compressive strength of 4000 psi (27,580 kPa).

Measuring losses in prestressed concrete requires accurately accounting for steel strains and helps ensure the accurate reporting of strains associated with prestress losses. Therefore, the elongation of the steel strands was observed, measured, and recorded at the time of stressing for the two beams where strains were measured. The results were as follows:

- Initial pretension of 1000 lb (4448 N) was placed on each individual strand. This effectively straightened the strand and allowed for the orderly tensioning of all strands. The strand strain at this stage was not directly measured because it is not possible to assess the amount of slack in the strand prior to the initial tensioning. At 1000 lb of preload tension, however, the strand strain would be approximately 160 microstrains.
- Each strand was marked with tape at the stressing end of the prestressing bed. The prestressing beds were each 440 ft (134 m) in length. The length of free strand from the dead end to the tape was approximately 430 ft (131 m).
- Each strand was individually tensioned to a total force of about 44,000 lb (195,712 N). This corresponds to 202.5 ksi (1396 MPa) or $0.75f_{pu}$ where f_{pu} is the specified minimum tensile strength of prestressing strand concrete members. Elongation was measured at 36 in. (914 mm) and photographs were taken for quality control. The strand strain at this stage was measured as 36 in./430 ft (914 mm/131 m), or 0.006980 in./in.
- Adding the two strains together gives a total prestress jacking strain of 0.007140 in./in. That strain, using modulus of prestressing steel E_{ps} = 28,500 ksi (193,000 MPa), gives a strand jacking stress of 203.4 ksi (1402 MPa).

In pretensioned concrete, strand and concrete remain bonded in the absence of cracking. Therefore, after beam fabrication, concrete and steel share the same strain deformations. Losses that occur after beam fabrication because of concrete volume changes subtract steel strains attained at pretensioning. These losses are all inclusive of total prestress loss, apart from the relaxation losses that occur in the steel. Relaxation losses cannot be measured by concrete strains and must be estimated from other models.

Results and discussion

Two prestressed beams, beam mark 27 (span 9) and beam mark 42 (span 14) were instrumented with VWSGs, bonded foil strain gauges, and thermocouples. Instrumentation was installed at midspan and end regions, but this paper and the topics related to prestress losses are affected only by measurements made at midspan. **Figure 4** shows the location of instrumentation at midspan of both beams. Data acquisition systems were solar powered with batteries continuously charged by solar panels. Continuous structural monitoring was performed through wireless technology that transmitted data from the instrumentation to data storage in real time. Since April 2020, the structural monitoring system has provided an ongoing stream of data from beam fabrication through concrete casting, form removal, detensioning, handling, storage, transit, erection, and construction of the bridge, continuing through the current in-service life of the SH 4 bridge. The strain data were collected from VWSGs located in the top flange 9.3 in. (236 mm) from the top of the beam, situated on the web 29.3 in. (744 mm) from the top of the beam, and in the bottom flange located near the center of gravity of the steel 48.5 in. (1232 mm) from the top of the beam. The actual strain measurements can be adjusted to compensate for the change in length of the vibrating wires due to temperature changes, or the effects of temperature can be included in the measurement. **Figure 5** shows the instrumentation installed at midspan of beam mark 27 before casting.

Measured concrete strains

When reporting losses from measured concrete strains, it is important to remember that temperatures can affect the strain measurement because concrete and steel both expand with increases in temperature. To demonstrate and report the temperature variations that occur at early ages, **Figure 6** shows measured concrete temperatures in the first 72 hours during fabrication of beam mark 27 (span 9). The ambient temperature at the time of casting was approximately 80˚F (27˚C). Maximum concrete temperatures occurred approximately 9 hours after casting. Maximum temperatures were measured at approximately 170˚F (77 ˚C) in the top flange and about 150˚F (66 ˚C) in the bottom flange. At detensioning, significant cooling had occurred and concrete temperatures ranged between 115˚F (46 ˚C) and 95˚F (35 ˚C).

Figure 7 reports concrete strains in the first 30 hours after concrete casting for beam mark 27. The strains reported in Fig. 7 have been adjusted to compensate for changes in temperature, so these values represent the measured concrete strains that can be directly related to prestress losses.

Figure 7 shows the changes in concrete strain that occurred at detensioning. For beam mark 27, detensioning occurred at approximately 23 hours after casting. Detensioning was performed by flame cutting individual strands over a time-frame of about 30 minutes. Strain readings indicated that the bottom flange compressive strain, located at the approximate center of gravity of the bottom strands, decreased from approximately 0.00 strain to about 950 microstrains. Compressive strains in the top flange were observed to increase from about 200 microstrains to about 600 microstrains.

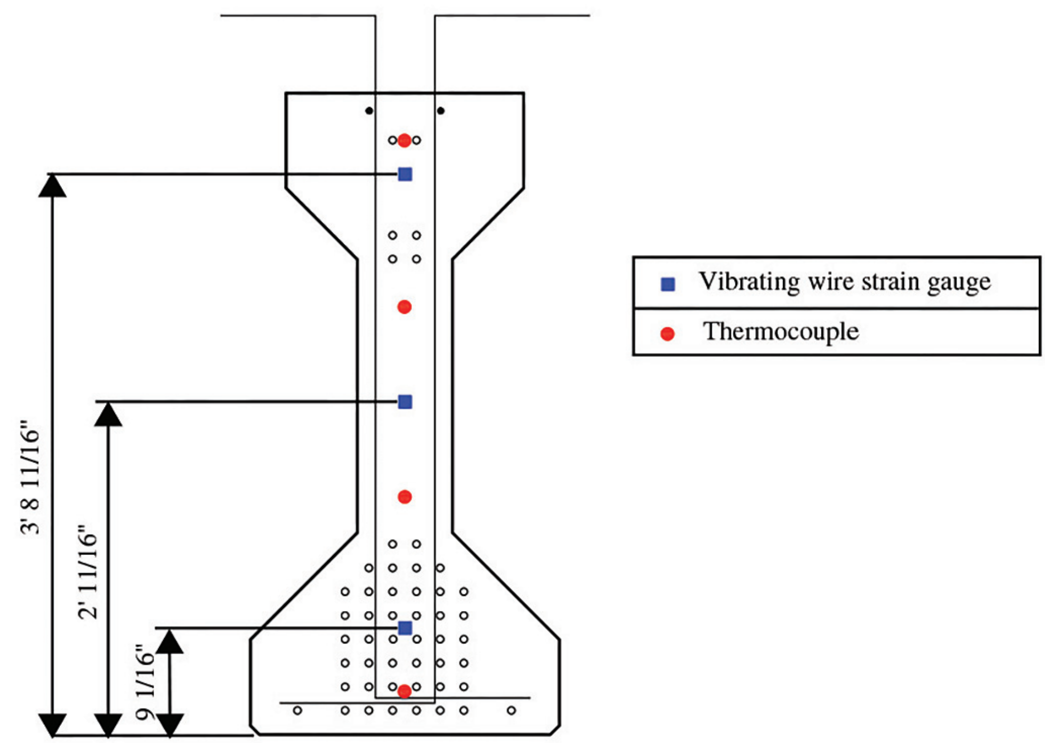

Figure 4. Instrumentation and instrument locations at midspan of beams mark 27, span 9 and mark 42, span 14. Note: 1” = 1 in. = 25.4 mm; 1’ = 1 ft = 0.305 m.

Figure 5. Photograph of instrumentation installed in reinforcement prior to casting for beam mark 27, span 9.

After the girders were removed from the prestressing bed, compressive strains slightly decreased in the top flange and slightly increased in the bottom flange. These strains indicate that a small frictional force was imposed on the precast concrete beam by the restraint of the prestressing bed. As the beam was lifted from the bed, that restraint disappeared, and additional curvature of the cross section was observed.[22]

Figure 8 reports the long-term strains measured on beam mark 27 and includes the time in days through 900 days (approximately 30 months). Beam mark 27 included mild reinforcement in the bottom flange. **Figure 9** reports the long-

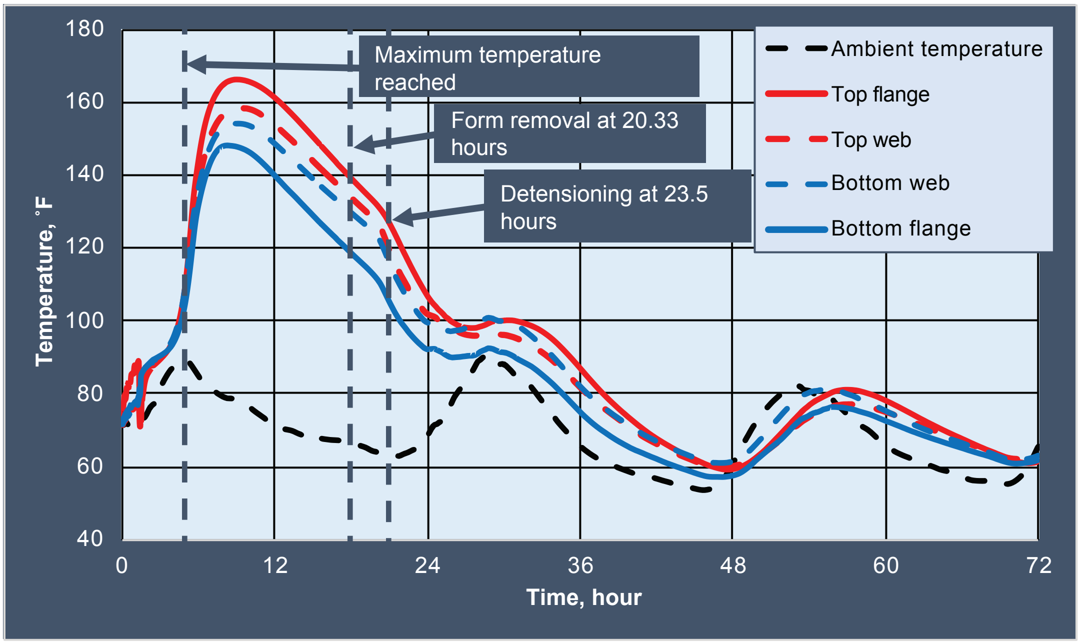

Figure 6. Concrete temperature at midspan from time prior to casting to 72 hours for beam mark 27, span 9. Note: °F = (°C × 1.8) + 32.

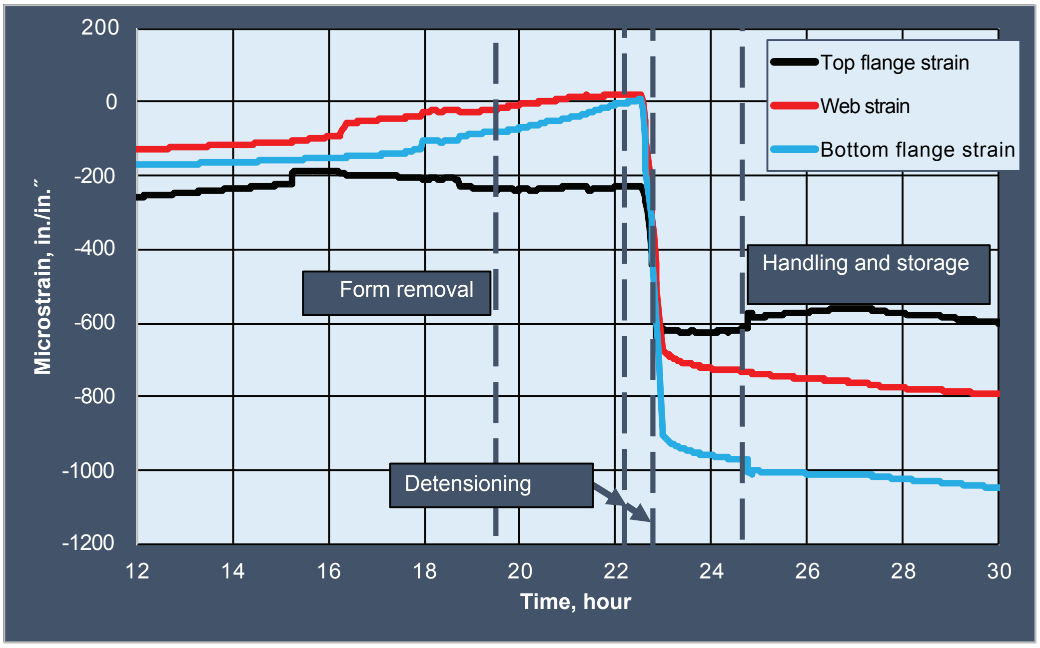

Figure 7. Measured concrete strain, temperature compensated, during detensioning for beam mark 27, span 9. Note: 1 in. = 25.4 mm.

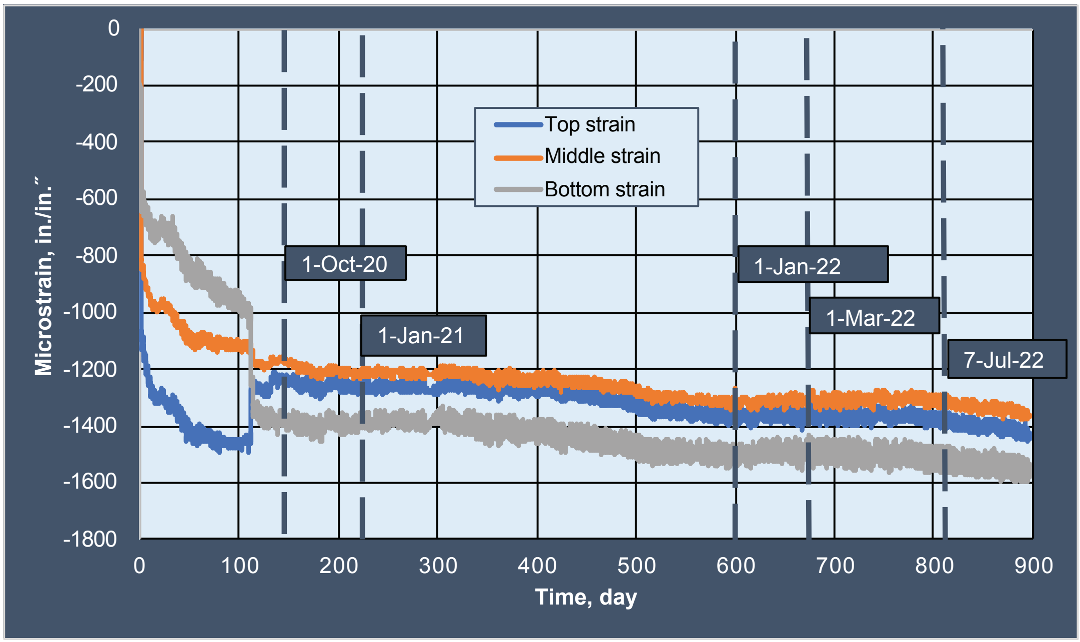

Figure 8. Measured concrete strains at midspan from fabrication to in-service life for beam mark 27, span 9.
Note: 1 in. = 25.4 mm.

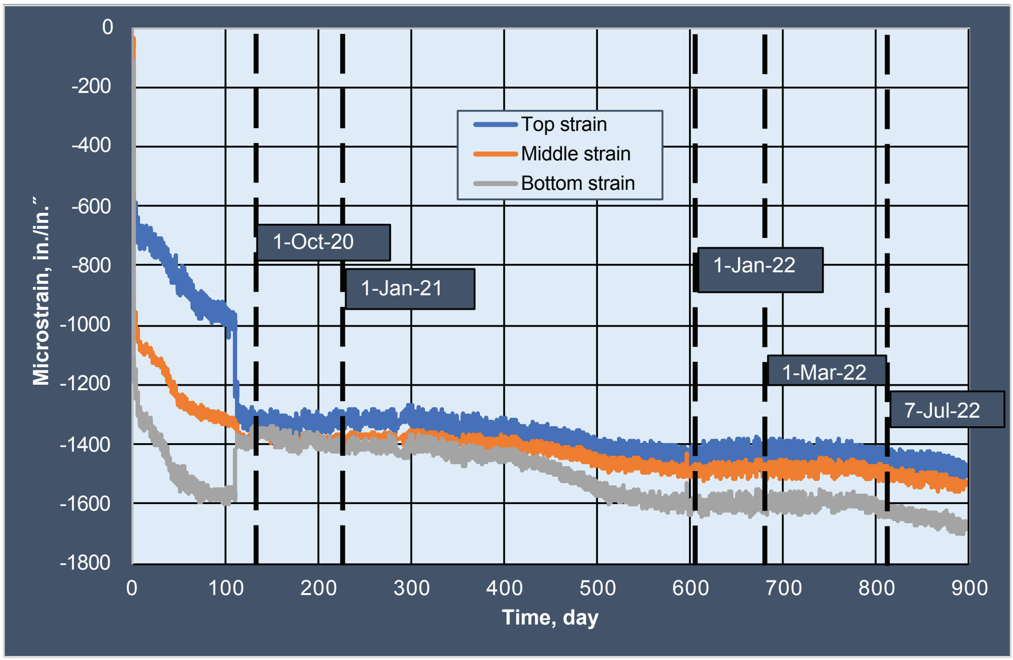

Figure 9. Measured concrete strain at midspan from fabrication to in-service life for beam mark 42, span 14.
Note: 1 in. = 25.4 mm.

term strains measured on beam mark 42 in span 14. Mark 42 did not include mild reinforcement in the bottom flange. Both beams were erected to the westernmost exterior girder position of their respective spans.

Observations include the following:

- In both beams, the initial compressive strains after detensioning were measured to be about -600 microstrains near the top flange and about -1000 microstrains in the bottom flange. Note that negative strains represent concrete compression.
- Strains measured immediately after release directly illustrate the effects of elastic shortening.
- For the time period after release and prior to slab casting, larger compressive strains are observed in the bottom flanges compared with those at the top flange, indicating that the beam is cambering upward.
- At early ages, concrete strains increased significantly. Within the first 110 days (from fabrication until slab casting), compressive strains in the top flange increased from approximately -600 to -1000 microstrains and compressive stresses in the bottom flange increased from approximately -1000 to -1450 microstrains in beam mark 27 and -1600 microstrains in beam mark 42. Both represent increases of strain in the range of 40% to 60%.
- Girders were transported and erected in May 2020 at 33 days (beam mark 27) and 34 days (beam mark 42) of age. From that point forward, the slope of changing strains began to decreased with time. This was observed from the date of hauling and erection until concrete deck slabs were cast.
- Both Fig. 8 and 9 show the effects from the dead load of fresh concrete when the deck slabs were cast at 112 and 113 days. Significant changes in strains occurred at slab casting; compressive strains in the top fibers increased, whereas compressive strains in the bottom fiber decreased. The fresh weight of the bridge deck concrete effectively closed the gap in compressive strains between the top of the bridge girder and the bottom. The decrease of variation in the measured strains from top to bottom represents a strain condition where the dead loads became effectively balanced by the prestressing

Table 2. Measured prestress losses

Time, days	Stage	Prestress losses* in beam mark 27, span 9, detail B with mild steel, ksi	Prestress losses* in beam mark 42, span 14, detail C without mild steel, ksi
0	Initialization and casting	0.0	0.0
1	Before release	-0.3	1.7
1	After release	23.8	25.2
3	After release	29.5	30.3
7	After release	31.8	33.4
14	Affter release	34.3	35.0
28	After release	35.1	36.1
33†/34‡	Hauling and erection	35.4	36.9
113†/112‡	Before deck slab cast	38.4	41.8
113†/112‡	After deck slab cast	34.5	37.8
526†/521‡	October 1, 2021	37.3	37.8
618†/613‡	January 1, 2022	38.3	42.1
677†/672‡	March 1, 2022	37.5	43.2
799†/794‡	July 1, 2022	37.9	42.4
900	October 15, 2022	39.4	43.0

Note: E_{ps} = modulus of prestressing steel. 1 ksi = 6.895 MPa.

† Beam mark 27, span 9.

‡ Beam mark 42, span 14.

* Prestress losses are the product of E_{ps} × concrete strain at the center of gravity of prestressed reinforcement.

moment. Note that load balancing is a common design practice in post-tensioned concrete but not prevalent (and rarely mentioned) in pretensioned concrete. Ideal load balancing can be defined as the point where the compressive strains become uniform through the depth of the cross section. Even though in composite precast concrete construction one will not observe uniform compression from load balancing, results like these where the strains at top and bottom nearly match after all dead loads are applied show that load balancing can still be employed to ensure effective design in precast, prestressed concrete. The effects of load balancing can be seen in Fig. 8 and 9 as the concrete strains come together at days 112 and 113.

- The average compressive strains over time increased after deck-slab casting, which indicates that volume changes in the prestressed concrete continued to cause prestress losses to increase over time.

Measured prestress losses

The prestress losses in the bridge girders were computed from the measured concrete strains, which were interpolated to find the concrete strain at the center of gravity of the prestressing strands. Total loss can be computed directly by multiplying the concrete strain at the center of gravity by the modulus of elasticity of the prestressing steel E_{ps}. E_{ps} is taken as 28,500 ksi (193,000 MPa). **Table 2** reports the measured prestress losses that were computed as described. Table 2 reports the losses from initial casting through 900 days. The losses reported here account only for losses associated with changes in concrete strain and do not include relaxation losses. They will, however, include elastic shortening, creep, shrinkage and any elastic gain that is achieved through application of dead loads, or volume changes in other bridge elements like the deck, parapets or diaphragms.

Over time, expected patterns for prestress losses emerged. **Figure 10** displays the prestress losses over time for both beam mark 27 and beam mark 42. Prestress losses are plotted on a logarithmic time scale that highlights the changes in strain that occurred at early ages while also displaying the time effects up to 900 days. At one day, the chart shows the large initial jump in prestress losses at 24 hours when the strands were detensioned. This jump in prestress losses is the result of elastic shortening. The elastic shortening for both beams is about 24 ksi.

Hauling (transportation) and erection on bridge bearings occurred at day 33 for beam mark 27 and day 34 for beam mark 42. From the initial detensioning until erection, prestress losses increased over time. The total prestress loss in beam mark 27 increased from 23.8 to 35.4 ksi (164 to 244 MPa, or 49%) and the total prestress losses in beam mark 42 increased from 25.2 to 36.9 ksi (174 to 254 MPa, or 46%).

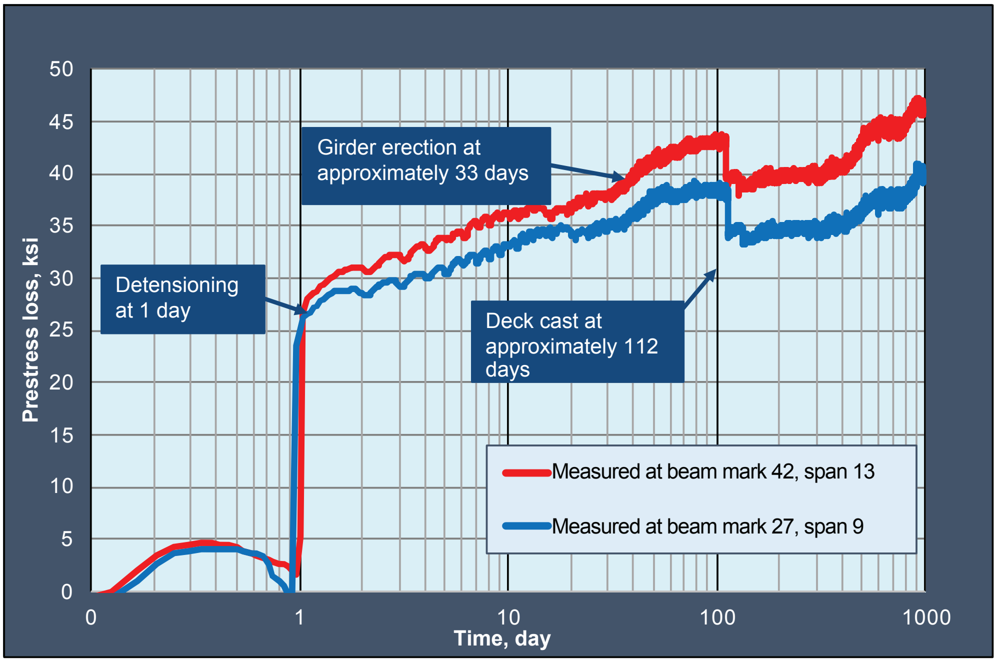

Figure 10. Measured prestress loss at midspan. of beam mark 27 and beam mark 42. Losses are computed from direct concrete strain measurements. Note: 1 ksi = 6.895 MPa.

From erection through slab casting, prestress losses continued to increase in both beam mark 27 and beam mark 42. Total prestress loss just prior to casting were measured to be 38.4 ksi in beam mark 27 and 41.8 ksi in beam mark 42, respectively. This represents an increase, beyond the initial elastic shortening, of 61% in beam mark 27 and 66% in beam mark 42. Note that beam mark 27 included four no. 7 mild steel reinforcing bars in the bottom flange and that beam mark 42 did not. Over time, prestress losses in beam mark 42 increase more than the losses in beam mark 27, and this measurable effect may be the direct result of the presence of mild reinforcement to help absorb time dependent volume changes causing prestress forces to shed from concrete to the mild reinforcement.

During slab casting, the measured prestress loss decreased in both beams. This was caused by the self-weight of the fresh concrete and the tension stresses the additional dead load causes to the bottom fibers of the precast concrete bridge beam. Measured losses show prestress loss decreased 3.9 ksi in beam mark 27 (from 38.4 ksi to 34.5 ksi) and prestress loss decreased 4.0 ksi in beam mark 42 (from 41.8 ksi to 37.8 ksi). This *decrease* in loss is the effective tensile stress in the steel caused as the precast concrete beam resists the self-weight of fresh concrete. The literature and historical syntax refer to this decrease in prestress losses as *elastic gain.*

After casting and hardening of the bridge deck slabs, which were made composite with the girders, the data show that prestress losses continued to increase. After deck slab casting and over the next two-plus years, prestress losses in beam mark 27 increased from 34.5 to 39.4 ksi (238 to 272 MPa). Similarly, prestress losses in beam mark 42 increased from 37.8 ksi to 43.0 ksi (262 to 296 MPa). Significantly, at the approximate age of 900 days, the total loss in beam mark 27 is 39.4 ksi (272 MPa) which is 19.5% of the initial jacking stress of 203.4 ksi. Total loss in beam mark 42 is 43.0 ksi [296 MPa], which is 21.1% of the initial jacking stress. Note that total loss in beam mark 42 is approximately 9% larger than that from beam mark 27. Note that beam mark 27 contains mild reinforcement in the bottom flange whereas beam mark 42 does not.

Estimating prestress losses

This paper estimated the prestress losses at the girder midspan using five different methods:

- 2020 AASHTO LRFD specifications, approximate method[1]
- 2020 AASHTO LRFD specifications, refined method[1]
- PCI Design Handbook method (based on Zia et al[23])
- Modified *PCI Design Handbook* method (using transformed cross-section properties instead of gross properties)
- Jayaseelan time-step method[2]

AASHTO approximate and refined methods The prestress losses computed using the AASHTO LRFD specifications' approximate method combines long-term losses from concrete creep, shrinkage, and relaxation of prestressing strands. This method utilizes the gross section properties, so the inclusion of mild reinforcing steel is not accounted for in the prestress loss calculations. The AASHTO LRFD specifications' refined method employs transformed cross-section properties. To compute losses at a specific age, the refined method uses time-dependent analysis by calculating the creep coefficient of concrete and shrinkage strain of concrete for both the girder and concrete deck at varying time intervals. Using the AASHTO refined method, prestress losses were calculated before deck casting at approximately 110 days and again for time t = 900 days. For the AASHTO methods, the initial modulus of elasticity E_{ci} or design modulus of elasticity E_c was estimated using AASHTO Eq. (5.4.2.4-1) with aggregate correction factor K_1 = 1.0:

$$E_c = 120{,}000 K_1 w_c^2 f_c'^{0.33} \quad \text{(AASHTO Eq. [5.4.2.4-1])}$$

where

w_c = unit weight of concrete

f_c' = concrete compressive strength

PCI Design Handbook The *PCI Design Handbook* method was first published by Zia et al. in 1979.23 This method estimates prestress losses using gross section properties that exclude the effects of mild reinforcement. This study also computed loses with a modified *PCI Design Handbook* method, which employs transformed section properties. Hale and Russell[13] showed that this was an effective means to estimate prestress losses. In this research and for the *PCI Design Handbook* method, the initial modulus of elasticity of concrete E_{ci} or design modulus of elasticity of concrete E_c was estimated using the following equation from ACI 363R.[24]

$$E_c = 40{,}000\sqrt{f_c'} + 1\times10^6 \text{ psi} \quad \text{(ACI 363R-10 Eq. [6-1])}$$

Jayaseelan time-step method Jayaseelan and Russell[2] proposed a time-step method for estimating day-to-day losses. This method evaluates the strength and modulus of concrete as a function of time, calculated daily. This method also utilizes transformed cross-section properties of the girder. Creep and shrinkage strains were analyzed independently and estimated based on models for creep and shrinkage found in ACI 209.[19] The method employs an "effective modulus" approach from a creep coefficient that is computed daily. In these estimates, the concrete age at transfer is 1 day and the time of deck casting was 110 days. Prestress losses at midspan were computed daily to 900 days. The Jayaseelan time-step method is useful to predict day-to-day losses and can be graphed to show the change in losses over time.

For this method, the initial modulus of elasticity of concrete E_{ci} or design modulus of elasticity of concrete E_c was estimated using the equation given in section 19.2.2.1a of the

American Concrete Institute's *Building Code Requirements for Structural Concrete (ACI 318-14) and Commentary (ACI 318R-14)*. The equation is given as follows:

$$E_c = 33w^{1.5}\left(f_c'\right)^{0.5} \quad \text{(ACI 318-14 Eq. [19.2.2.1.a])}$$

where

w = unit weight of concrete

Elastic shortening

The measured elastic shortening losses are reported in **Table 3**. The table also shows the concrete stresses at the center of gravity f_{cgp} immediately after detensioning. In Table 3, elastic shortening was derived directly from measured concrete strains and computed by multiplying the measured strains by the steel modulus. The concrete stress f_{cgp} was computed from equilibrium at the midspan, where the effec-

Table 3. Comparison of the derived modulus from the measured elastic shortening with different design equations

	Modulus of elasticity, ksi	Measured elastic shortening loss, ksi	f_{cgp}, ksi
AASHTO Eq. (5.4.2.4-1)	5132	n/a	n/a
ACI 363R-10 Eq. (6-1)	4347	n/a	n/a
ACI 318-14 Eq. (19.2.2.1a)	5072	n/a	n/a
Beam mark 27 (derived from concrete strains)	3846	24.1	3.25
Beam mark 42 (derived from concrete strains)	3914	23.5	3.23
ASTM C469 at 3 days, average	4090	n/a	n/a

Note: AASHTO = the American Association of State Highway and Transportation Officials; ACI = American Concrete Institute; f_{cgp} = sum of concrete stresses at the center of gravity of prestressing strands due to prestressing force at transfer and the self-weight of the member; n/a = not applicable. 1 ksi = 6.895 MPa.

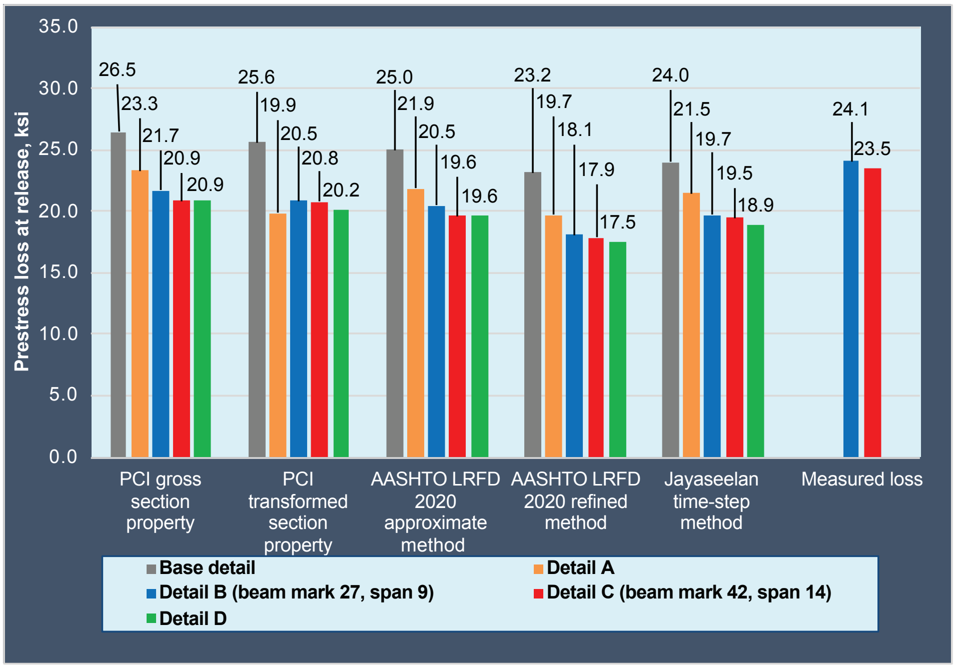

Figure 11. Prestress loss at release for measured loss and predicted loss using various prediction models. Note: AASHTO LRFD = the American Association of State Highway and Transportation Officials' *AASHTO LRFD Bridge Design Specifications*. 1 ksi = 6.895 MPa.

tive prestress force, after elastic shortening, must be balanced by concrete stresses. These calculations led directly to the computation for the initial elastic modulus of the concrete E_{ci}. Table 3 reports the measured E_{ci} along with E_{ci} values computed from the three different commonly used design equations. The data show that the commonly used design equations overpredict E_{ci} by up to 30%. These data indicate that the ACI 363R-10 equation 24 overpredicts the elastic modulus by up to 13%. It is important to note that the AASHTO LRFD specifications' equations for prestress losses were developed using conventional concrete, during a time prior to the widespread use of SCC. A common theme in the literature is that SCC tends to possess a lower elastic modulus than conventional concrete and this fact is demonstrated in these measurements.

These comparisons are also highlighted in **Fig. 11**, which charts the measured elastic shortening versus the losses predicted using the five different methods. It is notable that all the loss-prediction models underestimated the elastic shortening 10% to 20% of the measured elastic shortening for both beams. Whereas elastic shortening was 24.1 ksi for beam mark 27 and 23.5 ksi for beam mark 42, all of the predicted methods estimated elastic shortening at lower values with the AASHTO refined method underestimating it by the widest margin. This is because all of the various methods overestimate the concrete modulus at release, so, in turn the elastic shortening that results from the application of prestress force is underestimated. The overprediction of concrete modulus was observed in the early-age strain readings shown in Fig. 7.

Comparison of measured and estimated prestress losses over time

Figure 12 compares the prestress losses at 900 days that were estimated using the various prediction models with measured losses for beam mark 27 and beam mark 42. **Table 4** reports prestress losses at 110 days (the approximate day of slab casting) and 900 days.

It is important to note here that both the AASHTO LRFD specifications' approximate method and *PCI Design Handbook* methods cannot predict other interim time intervals. For methods that cannot predict losses at a specific time, the long-term losses were substituted into Table 4 and Fig. 12 for 900 days.

The AASHTO LRFD specifications' refined method overpredicted the losses in girder mark 27 by 2.2 ksi (15 MPa) and underpredicted the losses in beam mark 42 by 2.2 ksi compared with the measured losses. The Jayaseelan time-step method underestimated the prestress losses in mark 27 by 3.5 ksi (24 MPa) and underestimated losses for mark 42 by 8.6 ksi (59 MPa). However, any similarity in the loss estimations at 900 days should be tempered by the fact that the AASHTO LRFD specifications' methods significantly underpredicted elastic shortening but then overpredicted

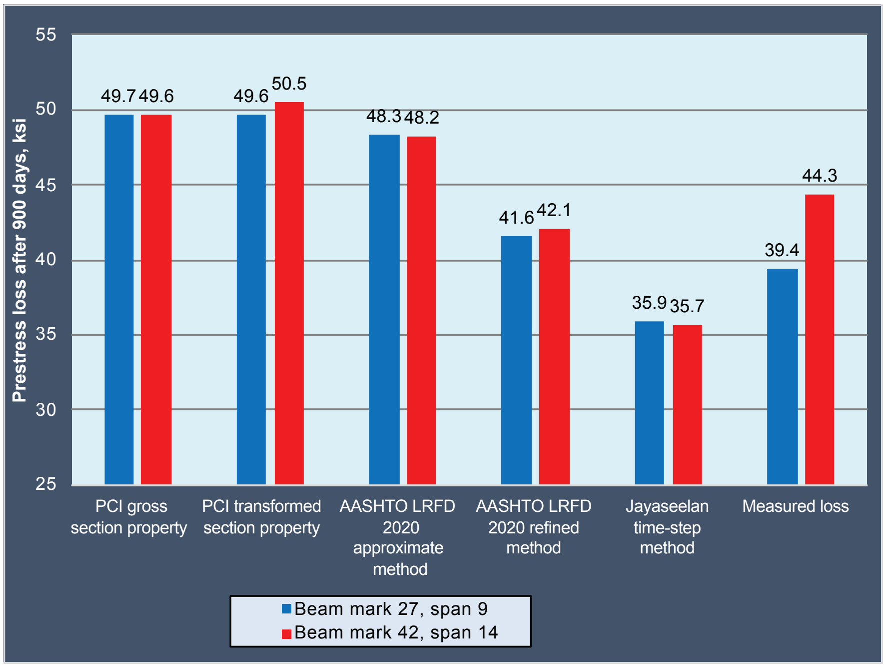

Figure 12. Prestress loss after 900 days for measured loss and predicted loss using various prediction models.
Note: AASHTO LRFD = the American Association of State Highway and Transportation Officials' *AASHTO LRFD Bridge Design Specifications*. 1 ksi = 6.895 MPa.

Table 4. Estimated prestress losses at midspan

Cross-section detail	Age, days	AASHTO LRFD 2020		*PCI Design Handbook*		Time-step method	Measured losses
		Approximate method	Refined method	Gross properties	Transformed properties		
Base	1	25.0	23.2	26.5	25.6	24.0	n/a
	110	n/a	47.4	n/a	n/a	43.9	n/a
	900	51.3	49.7	55.0	55.0	42.6	n/a
A	1	21.9	19.7	23.3	19.9	21.5	n/a
	110	n/a	42.1	n/a	n/a	40.2	n/a
	900	50.5	44.3	52.9	53.6	38.5	n/a
B	1	20.5	18.1	21.7	20.9	19.7	23.5
	110	n/a	39.5	n/a	n/a	37.3	38.4
	900	48.3	41.6	49.7	49.6	35.9	39.4
C	1	19.6	17.9	20.9	20.8	19.5	24.1
	110	n/a	39.4	n/a	n/a	37.2	41.8
	900	48.2	42.1	49.6	50.5	35.7	43.0
D	1	19.6	17.5	20.9	20.2	22.1	n/a
	110	n/a	38.7	n/a	n/a	36.4	n/a
	900	48.2	40.8	49.6	49.5	34.7	n/a

Note: AASHTO LRFD = the American Association of State Highway and Transportation Officials' *AASHTO LRFD Bridge Design Specifications*; n/a = not applicable. All values are in ksi. 1 ksi = 6.895 MPa.

the time-dependent losses. Similarly, the time-step method employed by Jayaseelan underpredicted elastic shortening and this underprediction persisted through the 900 days of measurement.

Figure 13 graphs the measured prestress losses and those estimated from the Jayaseelan time-step method. The Jayaseelan time-step method was used to determine prestress losses in both girders immediately after release at 24 hours, during storage, at girder installation on the bridge site, just prior to deck casting, right after deck casting, and after 900 days (approximately 800 days of in-service life). The trend of the loss prediction curve graphed using the Jayaseelan time-step method closely follows the measured losses for both girders mark 27 and 42. Figure 13 also plots the prestress losses that are predicted for the base case. The prediction model shows that the inclusion of fully tensioned top strands coupled with mild reinforcement reduces the prestress losses by approximately 6.3 ksi.

According to Table 4, the prestress losses estimated using different methods are significantly different. The AASHTO LRFD specifications' refined method is based on experiments with normal-strength concrete, and in this study, the predicted values of prestress losses using the AASHTO LRFD specifications' refined method were 2.4% larger than mark 27 and 8.7% lower than measured.

Comparison of measured losses and Jayaseelan time-step method with corrected modulus of elasticity

Results from Table 4 show that the overprediction of the elastic modulus led to the underestimation of the losses. One of the aims of this study is to evaluate the Jayaseelan time-step method. Therefore, the prediction method was repeated but using the corrected elastic moduli reported in Table 3. The initial modulus (at release) of elasticity of concrete E_{ci} was set to 3846 ksi (26,518 MPa) for mark 27, span 9 and 3914 ksi (26,987 MPa) for mark 42, span 14. Due to unavailability of substantial test data for the modulus of elasticity of the beams at later ages, the modulus of elasticity of the aging concrete E_c was estimated using ACI 363R-10 Eq. (6-1). This may have led to additional underestimation of losses over longer time periods. The Jayaseelan time-step method, when adjusted for the measured elastic modulus, provides an estimate for total prestress loss within 11% of that measured.

General comments regarding the estimation of prestress losses

One of the lessons that comes from this research, which is focused on the physical measurements of concrete temperatures and concrete strains at early and later ages, is that engineers,

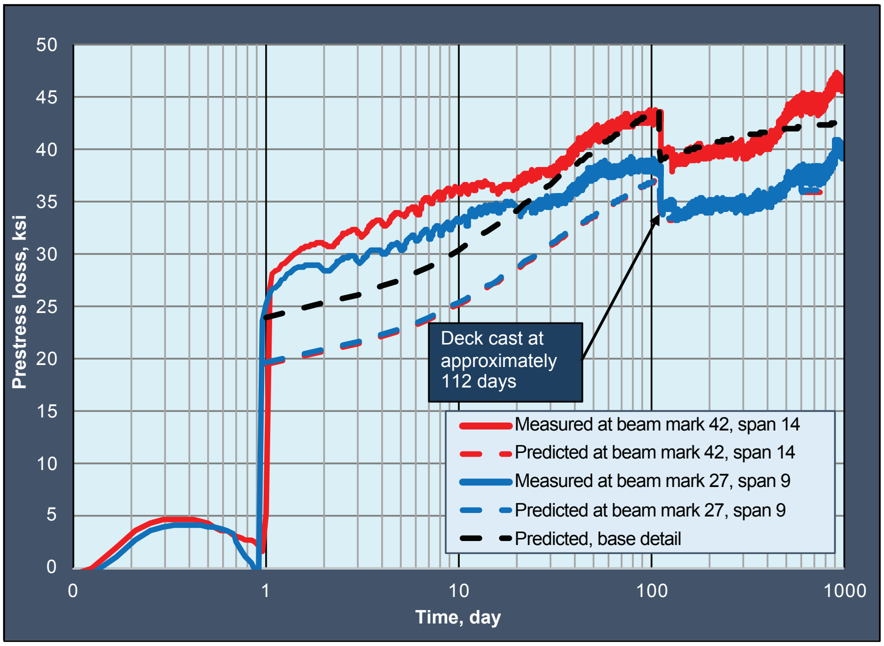

Figure 13. Prestress loss over time for both measured loss and predicted loss the Jayaseelan time-step method.
aNote: 1 ksi = 6.895 MPa.

designers, owners and fabricators should not place too much emphasis on the precise calculation of prestress losses from design calculations. Instead, these computations about prestress losses, despite best intentions and despite the appearance of precision (because of the detail and complication often found in those calculations), it may be best to remember that the calculation represents only an estimate. Therefore, the authors find common ground with the language of the past, which stated that the prestressed concrete industry (owners, fabricators, engineers, and constructors) recognized that we were merely estimating prestress losses and not performing precise calculations.

General comments regarding design choices: raising the center of gravity

Both of the prestressed concrete girders in which this study measured prestress losses were designed and built with prestressing strand patterns that raised the center of gravity of the prestressing steel and effectively reduced the prestressed moment. This was highlighted in Table 1, where the cross sections that had smaller eccentricity also had smaller prestressed moment. From Table 1, the base detail had the largest prestressed moment. That same detail goes on to exhibit the largest estimated prestress losses as shown in Table 4 (49.7 ksi [343 MPa] using the AASHTO LRFD specifications' refined method). The difference between the base detail and that of detail A (commonly used in Oklahoma) is estimated to be 5.4 ksi (37 MPa). The evidence from this relatively simple comparison as well as from other research shows clearly that the inclusion of fully tensioned top strands can effectively reduce prestress losses at least at the centroid of the prestressing force. Although it may be true that the total losses for strands in the bottom flange are unaffected by the inclusion of fully tensioned bottom strands, the engineer should remember that the total prestressing force is more balanced because the prestress forces in the top of the beam will not possess prestress losses as large as those for the bottom strands.

General comments regarding design choices—inclusion of mild steel as primary reinforcement

This research provides a direct comparison between two cross sections. Specifically, beam mark 27 contained mild reinforcement in the bottom flange, whereas beam mark 42 did not. The results from this direct comparison appear to be stark and clear. Both beams had similar initial elastic shortening losses and similar concrete strains at initial stages. However, over time, beam mark 27 experienced significantly smaller prestress losses. From the period of time beginning with detensioning to 900 days, the increase in prestress losses in beam mark 42, with no mild reinforcement, were significantly larger than the losses measured in beam mark 27. Beam mark 42 (without mild steel) increased losses 71%, by 17.8 ksi (123 MPa), to a total of 43.0 ksi (296 MPa), whereas mark 27 (with mild steel) increased losses 66%, by 15.6 ksi (108 MPa), to a total of 39.4 ksi (272 MPa). The authors recommend that engineers and fabricators consider the use of mild steel in the bottom flanges to help control prestress losses (and mitigate camber growth). Moreover, consider that the beam mark 42 had lower prestressed moment (Table 2). So, effectively, the inclusion of mild steel is effective at reducing long term losses even more than the direct comparison of the two cross section demonstrates.

General comments about SCC and prestress losses

The research shows that the total prestress losses were heavily influenced by larger-than-predicted elastic shortening losses. Elastic shortening was under-predicted because the SCC had approximately 15% to 33% lower elastic modulus than that predicted by design equations. Also, the preponderance of evidence in the literature indicates that the elastic modulus for SCC can be expected to be smaller than that of conventional, non-self-consolidating concrete. The change in material properties is significant and the changes should be considered when estimating prestress losses (and cambers). However, more research is needed where direct measurements of concrete strains and prestressed losses are made on beams that employ SCC. In the meantime, it seems prudent to adopt design details, such as the inclusion of mild steel and fully tensioned top strands, to help mitigate prestress losses and other serviceability problems that might result from total losses larger than predicted.

Conclusion

- The measured elastic modulus for SCC was 15% to 33% smaller than that predicted using commonly used design equations for elastic modulus. Because of this, the measured elastic shortening losses were underpredicted by similar percentages.
- Commonly used design equations that estimate elastic modulus appear to significantly overestimate the value of early-age concrete elastic modulus. This leads to significant underestimation of elastic shortening losses by 30% or more and underprediction of elastic shortening loss.
- The Jayaseelan time-step method, when used with the corrected modulus of elasticity of concrete, accurately predicted losses that were comparable to measured losses.
- The use of fully tensioned top prestressing strands reduced prestress losses by reducing the eccentricity of the prestressing force. Additionally, other prestressing patterns that raise the center of gravity of the prestressing force work in the same manner to reduce prestress losses.
- The Jayaseelan time-step method is a reliable method for estimation of prestress losses. However, underprediction of the elastic shortening at early ages resulted in underprediction of the losses at early ages.
- The elastic modulus for SCC is usually lower compared with conventional concrete. Overestimating the modulus of elasticity of concrete leads to underestimating the elastic shortening losses at an early age.
- A new equation that provides best accuracy for estimating elastic modulus for SCC should be developed for accurate estimation of prestress losses.
- The experimental data has shown that the losses can be reduced by incorporating a combination of top prestressing strands and mild steel in the bottom flange of the concrete girder bridge.
- The inclusion of mild reinforcement reduces the total prestress losses by approximately 10% in measured experimental data.
- The AASHTO LRFD specifications' refined method significantly underpredicts elastic shortening losses because the method uses common design equations for elastic modulus. Those equations overpredict the elastic modulus for SCC. Over time, the AASHTO refined method aligns more closely with measured values. This finding suggests that the AASHTO LRFD specifications' refined method inaccurately predicts both the short-term (elastic shortening loss) and long-term (creep and shrinkage) parts of prestressed losses. Therefore, this study finds that this method is inaccurate at both short-term and long-term estimates for the SCC used in these beams, and that the fact that predicted losses ended up within 10% of the measured losses is coincidental. The prestress loss equations in the AASHTO LRFD specifications should be revisited with more emphasis on producing losses from systematic measurement of hardened-material properties.

Recommendations

- Engineers, contractors, fabricators, and owners should consider the use of mild steel in the bottom flanges in order to help control prestress losses (and mitigate camber growth).
- Engineers, contractors, fabricators, and owners should consider inclusion of fully tensioned top strands as part of an overall strategy to control prestress losses. Quality assurance programs for concrete materials should include measurements of elastic modulus at early ages and at 28 days. These results should be communicated to engineers, contractors, and other stakeholders to assist in predicting prestress losses.
- In estimating prestressed losses, the elastic modulus used when estimating prestress losses should be derived from physical measurement of elastic modulus of concrete made from representative mixtures and representative constitutive materials.

- The AASHTO LRFD specifications' equations for prestress losses should be modified or changed to reflect the changes in the material properties of commonly used concrete.

References

1. AASHTO (American Association of State Highway and Transportation Officials). 2020. *AASHTO LRFD Bridge Design Specifications*. 9th ed. Washington, DC: AASHTO.

2. Jayaseelan, Hema, and Bruce W. Russell. 2019. "Reducing Cambers and Prestress Losses by Including Fully Tensioned Top Prestressing Strands and Mild Reinforcing Steel." *PCI Journal* 64 (3): 29–46. https://doi.org/10.15554/pcij64.3-05.

3. Okamura, Hajime, and Masahiro Ouchi. 1998. "Self-Compacting High Performance Concrete." *Progress in Structural Engineering and Materials* 1 (4): 378–383.

4. Erkmen, Bulent. 2008. "Self-Compacting Concrete for Prestressed Bridge Girders." PhD diss., University of Minnesota.

5. Rasekh, Haleh, Alireza Joshaghani, Soheil Jahandari, Farhad Aslani, and Maryam Ghodrat. 2020. "Rheology and Workability of SCC." In *Self-Compacting Concrete: Materials, Properties and Applications*, ed. Rafat Siddique, 31–63. Woodhead Publishing. https://doi.org/10.1016/B978-0-12-817369-5.00002-7.

6. Aggarwal, Paratibha, and Yogesh Aggarwal. 2020. "Strength Properties of SCC." In *Self-Compacting Concrete: Materials, Properties and Applications*, ed. Rafat Siddique, 83–115. Woodhead Publishing. https://doi.org/10.1016/B978-0-12-817369-5.00004-0.

7. Holschemacher, Klaus, and Yvette Klug. 2002. "A database for the evaluation of hardened properties of SCC." *Lacer* no. 7: 124–134.

8. García Theran, Mauricio M. 2008. "Experimental Evaluation of the Modulus of Elasticity of Self-Consolidating Concrete." MS thesis, University of Puerto Rico. https://hdl.handle.net/20.500.11801/1738.

9. ACI (American Concrete Institute) Committee 237. 2007. *Self-Consolidating Concrete*. ACI 237R-04. Farmington Hills, MI: ACI.

10. Myers, John J., Jeffery S. Volz, Eric Sells, Krista Porterfield, Trevor Looney, Brian Tucker, and Kyle Holman. 2012. *Self-Consolidating Concrete (SCC) for Infrastructure Elements*. Missouri Department of Transportation (MoDOT) project no. TRyy1103, report cmr 13-003. Jefferson City, MO: MoDOT.

11. Bonen, David, and Surendra P. Shah. 2005. "Fresh and Hardened Properties of Self-Consolidating Concrete." *Progress in Structural Engineering and Materials* 7 (1): 14–26. https://doi.org/10.1002/pse.186.

12. Alghazali, Hayder H., and John J. Myers. 2020. "Creep and Shrinkage of SCC." In *Self-Compacting Concrete: Materials, Properties and Applications*, ed. Rafat Siddique, 131–146. Woodhead Publishing. https://doi.org/10.1016/B978-0-12-817369-5.00006-4.

13. Hale, W. Micah, and Bruce W. Russell. 2006. "Effect of Allowable Compressive Stress at Release on Prestress Losses and on the Performance of Precast, Prestressed Concrete Bridge Girders." *PCI Journal* 51 (2): 14–25. https://doi.org/10.15554/pcij.03012006.14.25.

14. Saiidi, M., B. Douglas, and Shumin Feng. 1994. "Prestress Force Effect on Vibration Frequency of Concrete Bridges." *Journal of Structural Engineering* 120 (7): 2233–2241. https://doi.org/10.1061/(ASCE)0733-9445(1994)120:7(2233).

15. Liu, Xiucheng, Bin Wu, and Cunfu He. 2015. "A Novel Integrated Sensor for Stress Measurement in Steel Strand Based on Elastomagnetic and Magnetostrictive Effect." In *Engineering Asset Management—Systems, Professional Practices and Certification: Proceedings of the 8th World Congress on Engineering Asset Management (WCEAM 2013) & the 3rd International Conference on Utility Management & Safety (ICUMAS)*, ed. Peter W. Tse, Joseph Mathew, King Wong, Rocky Lam, and C. N. Ko, 65–73. Switzerland: Springer International Publishing. https://doi.org/10.1007/978-3-319-09507-3_7.

16. Chaki, S., and G. Bourse. 2009. "Stress Level Measurement in Prestressed Steel Strands Using Acoustoelastic Effect." *Experimental Mechanics*, no. 49: 673–681. https://doi.org/10.1007/s11340-008-9174-9.

17. Baran, Eray, Carol K. Shield, and Catherine E. French. 2005. "A Comparison of Methods for Experimentally Determining Prestress Losses in Pretensioned Prestressed Concrete Girders." In *Ned H Burns Symposium on Historical Innovations in Prestressed Concrete*, 161–180. ACI Special Publication 231. Farmington Hills, MI: ACI. https://doi.org/10.14359/14926.

18. Joint ACI-ASCE Committee 423. 2016. *Guide to Estimating Prestress Loss*. ACI (American Concrete Institute) 423.10R-16. Farmington Hills, MI: ACI. https://www.concrete.org/Portals/0/Files/PDF/Previews/423.10R-16_preview.pdf.

19. ACI 209R-92 (reapproved 2008). Prediction of Creep, Shrinkage, and Temperature Effects in Concrete Structures. Farmington Hills, MI: ACI.

20. Russell, Bruce W. 2018. “Using Fully Bonded Top Strands in Pretensioned Concrete Bridge Girders.” *Aspire* 12 (3): 26–28.

21. Oklahoma Department of Transportation. 2019. *Standard Specifications for Highway Construction*. https://oklahoma.gov/content/dam/ok/en/odot/documents/c_manuals/specbook/2019--full-spec-web-version.pdf.

22. Cook, Ronald A., David Bloomquist, and Jonathan E. Sanek. 2005. *Field Verification of Camber Estimates for Prestressed Concrete Bridge Girders*. Report BD-545 RPWO 7. Tallahassee, FL: Florida Department of Transportation.

23. Zia, Paul, H. Kent Preston, Norman L. Scott, and Edwin B. Workman. 1979. “Estimating Prestress Losses.” *Concrete International* 1 (6): 32–38.

24. ACI Committee 363. 2010. *Report on High Strength Concrete*. ACI 363R-10. Farmington Hills, MI: ACI.

25. ACI Committee 318. 2014. *Building Code Requirements for Structural Concrete (ACI 318-14) and Commentary (ACI 318R-14)*. Farmington Hills, MI: ACI.

Notation

e = eccentricity of the prestressing strand

E_c = design modulus of concrete at detensioning

E_{ci} = initial modulus of concrete at detensioning

E_{ps} = modulus of prestressing steel

f_{cgp} = sum of concrete stresses at the center of gravity of prestressing strands due to prestressing force at transfer and the self-weight of the member

f_{pu} = specified minimum tensile strength of prestressing strand concrete members

F_{se} = effective prestressing force in the strands after losses

f'_c = concrete compressive strength

K_1 = a correction factor for the source of aggregate to be taken as 1.0

t = time

w = unit weight of concrete

w_c = unit weight of concrete

About the authors

Alla Eddine Acheli, PhD, is a graduate engineer with Walter P. Moore in Houston, Tex. He completed his PhD in civil engineering at Oklahoma State University in Stillwater, Okla., in 2023.

Hema Jayaseelan, PhD, PE, is an assistant professor of civil engineering at Cedarville University in Cedarville, Ohio. She earned her doctorate and master's degree in civil engineering from Oklahoma State University.

Bruce W. Russell, PhD, PE, SE, FACI, is a professor of civil and environmental engineering at Oklahoma State University in Stillwater, Okla. He has been a PCI member since 1990 and currently serves on the PCI Committee on Bridges, Concrete Materials Committee, and Prestressed Reinforcement Committee.

Walter Peters, PE, is an assistant bridge engineer for the Oklahoma Department of Transportation. Over a 51-year career, he has worked as a bridge designer, project engineer, and assistant bridge engineer. Peters has a BS degree in civil engineering from Texas Tech University in Lubbock, Tex.

Chris Filip is a structural engineer in training at the Wallace Design Collective in Tulsa, Okla. He completed his MS at Oklahoma State University in 2022 and has been practicing for two years.

Abstract

This study investigates prestress loss measured on precast, prestressed concrete bridge beams for a bridge in Oklahoma. The research examines the effects of including mild reinforcing steel in the bottom flange of precast concrete girder and the alternative prestressing pattern on the prestressing losses of pretensioned bridge girders. Using solar powered batteries, a structural monitoring system has been providing an ongoing stream of data since beam fabrication and will continue through the service life of the bridge. In addition to the measured data, the prestress losses were predicted at the girder midspan using five different methods for computing prestress loss. Data show that current equations overestimate the concrete elastic modulus at early ages, leading to an underprediction of elastic shortening losses. Results show that prestress losses are reduced by incorporating a combination of fully tensioned top strand plus mild steel in the bottom flanges of the bridge girder.

Keywords

Mild-steel reinforcement, prestress loss, self-consolidating concrete, time-step method, vibrating wire strain gauge.

Review policy

This paper was reviewed in accordance with the Precast/Prestressed Concrete Institute's peer-review process. The Precast/Prestressed Concrete Institute is not responsible for statements made by authors of papers in *PCI Journal*. No payment is offered.

Publishing details

This paper appears in *PCI Journal* (ISSN 0887-9672) V. 69, No. 5, September–October 2024, and can be found at https://doi.org/10.15554/pcij69.5-03. *PCI Journal* is published bimonthly by the Precast/Prestressed Concrete Institute, 8770 W. Bryn Mawr Ave., Suite 1150, Chicago, IL 60631.

Reader comments

Please address any reader comments to *PCI Journal* editor-in-chief Tom Klemens at tklemens@pci.org or Precast/Prestressed Concrete Institute, c/o *PCI Journal*, 8770 W. Bryn Mawr Ave., Suite 1150, Chicago, IL 60631.